Rapid Communications

Super-Arrhenius behavior of molecular glass formers

Ankit Singh and Yashwant Singh
Department of Physics, Banaras Hindu University, Varanasi-221 005, India

(Received 10 November 2018; published 7 March 2019)

A theory is developed to calculate values of the potential-energy barriers to structural relaxation in molecular glass formers from the data of static pair-correlation function. The barrier height is shown to increase due to an increase in the number of "stable bonds" a particle forms with its neighbors and the energy of each bond as liquids move deeper into the supercooled (supercompressed) region. We present results for a system of hard spheres and compare calculated values of the structural relaxation time with experimental and simulation results.

DOI: 10.1103/PhysRevE.99.030101

The structural relaxation time of a molecular glass former grows by many orders of magnitude over a small range of temperatures when the system is cooled close to the glass transition temperature [1]. The glass transition is linked to dynamical arrest caused by particles being trapped in cages formed by their nearest neighbors [2,3]. It is widely accepted that the dynamics close to the glass transition is dominated by activation [4]. If the potential-energy barriers to relaxation were constant in temperatures, the relaxation time would follow the Arrhenius law. The super-Arrhenius behavior suggests that the potential-energy barriers in molecular glass formers increase with decreasing temperature and increasing density. The ubiquity of the phenomenon, irrespective of molecular details, points to a collective or cooperative behavior characterized by a length scale that grows as one approaches the glass transition. Beginning at least from Adam and Gibbs [5] who introduced the concept of "cooperatively rearranging regions" in the mid-1960s, many microscopic models [6–11] have been developed to uncover the physical mechanism behind growth of the cooperative length scale. One of the issues has been to define and determine objectively such a length scale [10–12], and relate it with the potential-energy barrier.

In dealing with classical many-body particle systems one often integrates out the kinetic energy of particles and considers only the potential energy of interactions in framing a theory or in simulations. In this Rapid Communication we show that when kinetic energy is allowed to compete with the effective potential energy felt by particles in a system, a new way of understanding the properties of dense systems emerges. Such an idea was first proposed by Hill [13] and used by Stogryn and Hirschfelder [14] and others [15] to describe the equilibrium and transport properties of gases.

A particle in a dense system feels a potential-energy barrier created by its neighbors. Depending upon the height of the barrier and the relative momenta of the surrounding particles, the central particle may get trapped and bonded (defined below) with neighboring particles. A particle whose total energy is higher than the barrier moves freely and collides with other particles. The concentration of these particles depends on density and temperature; the potential barrier becomes higher on increasing the density and lowering the temperature, and the kinetic energy of particles decreases on decreasing the temperature. A molecular liquid at high densities and low temperatures can therefore be considered as a network of particles connected with each other by (nonchemical) bonds with some free particles which move around and collide with other particles. Depending upon bonding energies, the lifetime of bonds may vary from microscopic to macroscopic time. When a particle dissociates from the network either by collision or by thermal activation, it may initiate breaking of neighboring bonds and creating a dynamical active domain [16,17]. The precipitous onset of slowness can be associated with the increasing number of bonds and the larger bond energy with which particles are bonded with neighbors.

One way to find the number of bonds formed by a particle with its neighbors is to use the data of static pair-correlation function. The theory we describe is applicable to all those systems for whose values of pair-correlation function in a supercooled (supercompressed) region are available. Here we consider a system of hard spheres and use the data of the radial distribution function (RDF) evaluated from an approximate integral equation theory [18] (our aim here is to show usefulness of the theory rather than numerical rigor).

In the case of a system of hard spheres where potential is zero when particles do not overlap and infinite otherwise, temperature becomes irrelevant apart from rescaling quantities; the natural control parameter is the packing fraction $\eta = \frac{\pi}{6}\rho\sigma^3$, where ρ is number density and σ is particles diameter. Experimentally, hard-sphere systems are obtained using colloidal particles [19], emulsions, or granular materials [20]. The fluid-crystal transition takes place at $\eta = 0.494$ and the melting transition at $\eta = 0.545$. When the system is compressed following a protocol which avoids crystallization, the structural relaxation time τ_α increases rapidly showing super-Arrhenius behavior. Whether τ_α diverges at a density lower than the random close-packed density, $\eta_{\rm rcp}(\simeq 0.64)$ or not is still a highly debated issue [21–23]. Kinetic arrest must occur at $\eta_{\rm rcp}$ because all particles block each other at that density.

The RDF $g(r)$ of a homogeneous and isotropic system consisting of particles of mass m in the center-of-mass

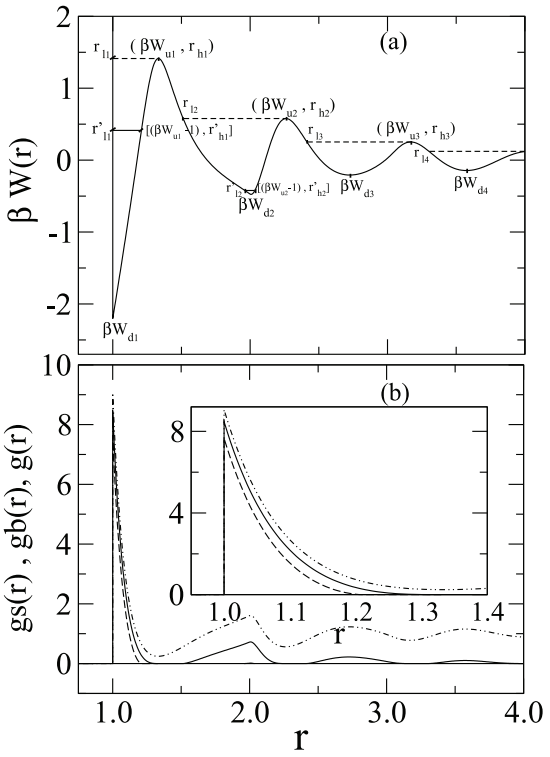

FIG. 1. (a) The reduced effective potential $\beta W(r)$ between a pair of particles separated by distance r (expressed in units of hard-sphere diameter σ) in a system of hard spheres at a packing fraction $\eta = 0.59$. $\beta W_{ui}, r_{hi}$ are, respectively, value and location of the ith maximum and r_{li} is the location on the left-hand side of the shell where $\beta W_i(r) = \beta W_{ui}$ (shown by a dashed line). The locations r'_{li} and r'_{hi} are values of r on the left- and the right-hand sides of the shell where $\beta W_i(r) = \beta W_{ui} - 1$ (shown by a solid line). βW_{di} is the depth of the ith shell. (b) Radial distribution functions $g(r)$ (dash-dotted line), $g_b(r)$ (solid line) and $g_s(r)$ (dashed line) vs r at $\eta = 0.59$. The various peaks correspond to various shells around a central particle. While $g(r)$ oscillates around one, $g_b(r)$ and $g_s(r)$ become zero at boundaries defined by (r_{li}, r_{hi}) for $g_b(r)$ and (r'_{li}, r'_{hi}) for $g_s(r)$. In the inset we show how values in the first shell differ from each other.

coordinates can be written as

$$g(r) = \left(\frac{\beta}{2\pi\mu}\right)^{3/2} \int d\mathbf{p}\, e^{-\beta[(p^2/2\mu)+W(r)]}, \tag{1}$$

where $\beta = (k_B T)^{-1}$ is the inverse temperature measured in units of the Boltzmann constant k_B and $\mathbf{p}$ is the relative momentum of a particle of mass $\mu = m/2$. The effective potential $W(r) = -k_B T \ln g(r)$ [24] is the sum of the (bare) pair potential and the system-induced potential energy of interaction between a pair of particles separated by distance r. In Fig. 1 we plot $\beta W(r)$ for a system of hard spheres at $\eta = 0.59$ as a function of r expressed in units of σ. The curve has several maxima and minima. We denote a region between two maxima $i-1$ and i ($i \geqslant 1$) as the ith shell and the minimum of the shell by βW_{di}. The value of the ith maximum is denoted by βW_{ui} and its location by r_{hi}.

All particles of the ith shell whose energies are less or equal to βW_{ui}, i.e., $\beta[\frac{p^2}{2\mu} + W_i(r)] \leqslant \beta W_{ui}$, get confined in the shell and can be considered to be bonded with the central particle.

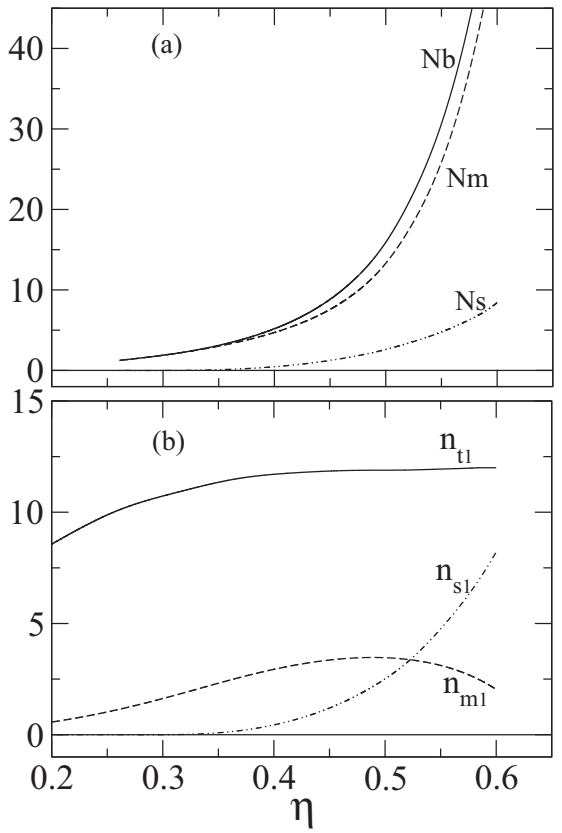

FIG. 2. (a) Number of total bonds N_b, metastable bonds N_m, and stable bonds N_s formed by a particle in a system of hard spheres vs packing fraction η. (b) Number of total particles n_{t1}, metastably bonded particles (m particles) n_{m1}, and stably bonded particles (s particles) n_{s1} in the first shell. The number n_{s1} increases rapidly and crosses n_{m1} at $\eta \simeq 0.524$. At $\eta = 0.524$ the crossover from nonactivated to activated dynamics takes place, due to the formation of cage by s particles.

The contribution made to $g(r)$ by these particles is

$$g_{bi}(r) = 4\pi\left(\frac{\beta}{2\pi\mu}\right)^{3/2} e^{-\beta W_i(r)} \int_0^{\sqrt{2\mu[W_{ui}-W_i(r)]}} e^{-\beta p^2/2\mu} p^2 dp$$
$$= e^{-\beta W_i(r)}\, \frac{\Gamma\left\{\frac{3}{2}, \beta[W_{ui} - W_i(r)]\right\}}{\Gamma\left(\frac{3}{2}\right)}, \tag{2}$$

where $\Gamma(m, n)$ is the incomplete gamma function and $W_i(r)$ is the effective potential of the ith shell in the range $r_{li} \leqslant r \leqslant r_{hi}$. Here r_{li} is the value of r where $\beta W_i(r_{li}) = \beta W_{ui}$ on the left-hand side of the shell (see Fig. 1). In Fig. 1(b) we plot $g(r)$ and $g_b(r)$ as a function of r at $\eta = 0.59$. The number of bonded particles of the ith shell at packing fraction η is

$$n_{bi}(\eta) = 24\eta \int_{r_{li}}^{r_{hi}} g_{bi}(r) r^2 dr. \tag{3}$$

The total number of particles bonded with the central particle is $N_b(\eta) = \sum_i n_{bi}(\eta)$. As shown in Fig. 2(a) by a solid line, N_b increases rapidly above the freezing density. This is due to an increase in the number of shells that surround the central particle and values of βW_{ui} and βW_{di} with η. It may, however, be noted that these particles (or bonds)

are embedded in a system which is equipped with thermal energy k_BT. Therefore, all those particles whose energies lie between $\beta W_{ui} - 1$ and βW_{ui} may not remain bonded for long due to thermal fluctuations; the lifetime depends on the bonding energy. We call these particles metastably bonded (henceforth referred to as m particles) and those particles whose energies lie between βW_{di} and $\beta W_{ui} - 1$, stably bonded (henceforth referred to as s particles). Most particles of N_b shown in Fig. 2(a) surrounding the central particle over a length of the pair-correlation function are m particles with bond energies much smaller than the thermal energy and are therefore transient.

The contribution made to $g(r)$ by the s particles of the ith shell is

$$g_{si}(r) = 4\pi\left(\frac{\beta}{2\pi\mu}\right)^{3/2} e^{-\beta W_i(r)} \int_0^{\sqrt{2\mu[W_{ui}-k_BT-W_i(r)]}} \times e^{-\beta p^2/2\mu} p^2 dp, \quad (4)$$

where $W_i(r)$ is in the range $r'_{li} \leqslant r \leqslant r'_{hi}$. Here r'_{li} and r'_{hi} are, respectively, values of r on the left- and the right-hand sides of the shell where $\beta W_i(r) = \beta W_{ui} - 1$ (see Fig. 1). We show values of $g_s(r)$ vs r in Fig. 1(b) by a dashed line for $\eta = 0.59$. The number of s particles with which the central particle is bonded, is

$$N_s(\eta) = \sum_i n_{si}(\eta); \quad n_{si}(\eta) = 24\eta \int_{r'_{li}}^{r'_{hi}} g_{si}(r) r^2 dr. \quad (5)$$

We plot N_s vs η in Fig. 2(a) along with N_b and $N_m = (N_b - N_s)$.

To understand why above a certain density a particle gets trapped by a stiff barrier and there is a crossover from nonactivated to activated dynamics, we examine the nature of particles of the first shell surrounding the central particle as a function of η. In Fig. 2(b) we plot the number of total particles n_{t1}, m particles n_{m1}, and s particles n_{s1}. We note that n_{t1} reaches the maximum value 12 at a density lower than the freezing density where most particles are still free. The number of m particles n_{m1} first increases and after reaching a maximum value ($\simeq$3) at $\eta \simeq 0.50$ starts decreasing and crosses n_{s1} at $\eta \simeq 0.524$, The number of s particles (n_{s1}) which build up the potential-energy barrier increases rapidly on increasing the density. We therefore consider $\eta = 0.524$ as the density which separates the two distinct dynamical domains. As for $\eta < 0.524$, the potential barrier is inconsequential and the activation is not the main mechanism of relaxation; the dynamics can be described by the mode coupling theory [25]. The activated dynamics becomes dominant for $\eta \geqslant 0.524$ when the central particle gets surrounded by an increasing number of s particles and the barrier starts caging the particle.

The potential-energy barrier to relaxation (activation energy) is assumed to be equal to the energy with which a particle is bonded with s particles. Thus the activation energy,

$$\beta E_s(\eta) = 24\eta \sum_i \int_{r'_{li}}^{r'_{hi}} [\beta W_{ui} - \beta W_i(r)] g_{si}(r) r^2 dr. \quad (6)$$

Here the bonding energy of each bond is measured from the barrier height.

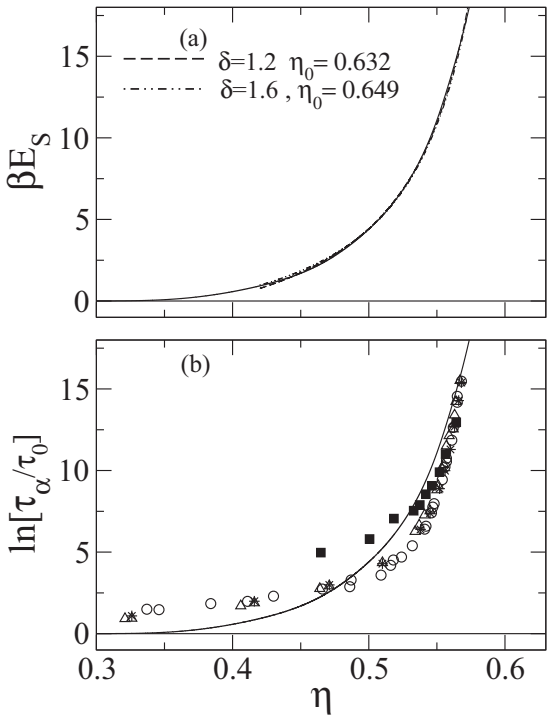

FIG. 3. (a) The potential-energy barrier (activation energy) βE_s vs η. Values found from the expression $\beta E_s(\eta) = A + \frac{B}{(\eta_0-\eta)^\delta}$ with (i) $\delta = 1.2$, $\eta_0 = 0.632$ (dashed line) and (ii) $\delta = 1.6$, $\eta_0 = 0.649$ (dash-dotted line) are compared with the calculated values. (b) Calculated values (solid line) of $\ln[\frac{\tau_\alpha}{\tau_0}]$ are compared with experimental values (filled square [26] and open circles [27]) and simulation values (open triangles [27] and stars [28]). The values of Refs. [27,28] are shifted to lower density by an amount $\Delta\eta = 0.03$.

In Fig. 3(a) we plot $\beta E_s(\eta)$ vs η and note that βE_s increases sharply for $\eta > 0.524$. The energy βE_s can be considered as the activation energy in the Arrhenius law, $\tau_\alpha(\eta) = \tau_0 \exp[\beta E_s(\eta)]$ where τ_0 is a microscopic timescale. Out of different functional forms used to fit the data of $\beta E_s(\eta)$, the best fit was found for $\beta E_s(\eta) = A + \frac{B}{(\eta_0-\eta)^\delta}$. In Fig. 3(a) we compare values found with (i) $\delta = 1.2$, $\eta_0 = 0.632$ and (ii) $\delta = 1.6$, $\eta_0 = 0.649$; both sets give equally good fit but while one set gives a value of η where τ_α diverges, lower, the other is higher than $\eta_{\rm rcp}$ (=0.64) indicating a limitation of such fitting. We emphasize that the fit shown in Fig. 3(a) does not necessarily favor the Vogel-Fulcher-Tammann law over other laws of relaxation as the low-density data where nonactivated dynamics mainly contributes to relaxations are not included in the fitting.

In Fig. 3(b) we compare our results of τ_α with experimental results reported for colloidal hard spheres in Refs. [26,27] and simulation results reported in Ref. [28]. It may, however, be noted that while our result is for a monodisperse system, the simulation result [28] is for a 50:50 binary mixture with diameters σ and 1.4σ and the experimental results are for polydisperse systems with polydispersity, s, of about 6% in [26] and above 10% in [27]. From simulation studies [29–31] it has been found that while moderately disperse hard spheres ($s \sim 5\%$–6%) behave almost like a monodisperse system, systems with larger dispersity ($s \gtrsim 10\%$) behave in a

complex way. One such effect is to move the glass transition to higher η. The unusual aging behavior due to strong decoupling between small and large spheres for $\eta > 0.59$ has also been observed [31,32]. The experimental [27] and simulation [27,28] data plotted in Fig. 3(b) are shifted to lower density by an amount $\Delta\eta = 0.03$, whereas the experimental values taken from Ref. [26] are plotted (shown by filled squares) without any shift. It may be noted that while the shifted values of Refs. [27,28] are in good agreement with the values of Ref. [26] for $\eta > 0.53$, a considerable difference remains in their values for $\eta < 0.53$. This suggests the need for more experimental data of moderately disperse systems [33]. The theoretical values shown by the solid line in the figure is in good agreement with these data for $\eta \gtrsim 0.50$; agreement for $\eta \lesssim 0.50$ is not expected as the dynamics in this region as argued above, is other than activation which has not been considered.

In summary, we developed a theory to calculate the potential-energy barriers to structural relaxation in a molecular glass former from the data of static pair-correlation function. A particle in a molecular liquid in the supercooled (supercompressed) region gets localized by forming (nonchemical) "stable bonds" with neighboring particles. The number of bonds and the bonding energy increase on lowering the temperature and increasing the density. The barrier height (activation energy) is equal to the energy βE_s with which a particle is bonded with the s particles. When βE_s is substituted in the Arrhenius law, a super-Arrhenius feature emerges. Using values of the radial distribution function for a system of hard spheres found from an approximate integral equation theory [18], we calculated the activation energy. The calculated values of τ_α are found to be in agreement with the experimental and simulation data in the region where activated dynamics is dominant.

We acknowledge financial help from the Council of Scientific and Industrial Research and the Indian National Science Academy, New Delhi.

[1] C. A. Angell, Science **267**, 1924 (1995); P. G. Debenedetti and F. H. Stillinger, Nature (London) **410**, 259 (2001).
[2] W. K. Kegel and A. van Blaaderen, Science **287**, 290 (2000).
[3] Z. Brown, M. J. Iwanicki, M. D. Gratale, X. Ma, A. G. Yodh, and P. Habdas, Europhys. Lett. **115**, 68003 (2016).
[4] M. Goldstein, J. Chem. Phys. **51**, 3728 (1969).
[5] G. Adam and J. H. Gibbs, J. Chem. Phys. **43**, 139 (1965).
[6] T. R. Kirkpatrick, D. Thirumalai, and P. G. Wolynes, Phys. Rev. A **40**, 1045 (1989).
[7] F. Ritort and P. Sollich, Adv. Phys. **52**, 219 (2003).
[8] T. R. Kirkpatrick and D. Thirumalai, Rev. Mod. Phys. **87**, 183 (2015).
[9] D. Chandler, J. P. Garrahan, R. L. Jack, L. Maibaum, and A. C. Pan, Phys. Rev. E **74**, 051501 (2006).
[10] L. Berthier, G. Biroli, J.-P. Bouchaud, W. Kob, K. Miyazaki, and D. R. Reichman, J. Chem. Phys. **126**, 184504 (2007).
[11] S. Whitelam, L. Berthier, and J. P. Garrahan, Phys. Rev. Lett. **92**, 185705 (2004); G. Biroli and J. P. Garrahan, J. Chem. Phys. **138**, 12A301 (2013).
[12] M. D. Ediger and P. Harrowell, J. Chem. Phys. **137**, 080901 (2012).
[13] T. L. Hill, *Statistical Mechanics* (McGraw-Hill, New York, 1956), Chap. 5; J. Chem. Phys. **23**, 617 (1955).
[14] D. E. Stogryn and J. O. Hirschfelder, J. Chem. Phys. **31**, 1531 (1959); **31**, 1545 (1959).
[15] Y. Singh, S. K. Deb, and A. K. Barua, J. Chem. Phys. **46**, 4036 (1967).
[16] P. Harrowell, Phys. Rev. E **48**, 4359 (1993); D. N. Perera and P. Harrowell, *ibid.* **54**, 1652 (1996).
[17] J. P. Garrahan and D. Chandler, Phys. Rev. Lett. **89**, 035704 (2002).
[18] S. L. Singh, A. S. Bharadwaj, and Y. Singh, Phys. Rev. E **83**, 051506 (2011). The Ornstein-Zernike equation along with the Roger-Young [F. J. Rogers and D. A. Young, Phys. Rev. A **30**, 999 (1984)] closure relation is found to give values of $g(r)$ reasonably accurate in the fluid region. It however, fails to capture features such as the split-second peak in the supercompressed region. Because of this we limit our calculation for $\eta \leqslant 0.60$. To check the accuracy we calculated the value of $Z = \frac{\beta P}{\rho}$ at $\eta = 0.597$ and found that the value is 24.2, which compares well with the exact value 25.3.
[19] P. N. Pusey and W. van Megen, Nature (London) **320**, 340 (1986).
[20] *Jamming and Rheology: Constrained Dynamics on Microscopic and Macroscopic Scales*, edited by A. J. Liu and S. R. Nagel (Taylor & Francis, New York, 2001).
[21] A. Donev, F. H. Stillinger, and S. Torquato, Phys. Rev. Lett. **96**, 225502 (2006).
[22] V. A. Martinez, G. Bryant, and W. van Megen, Phys. Rev. Lett. **101**, 135702 (2008).
[23] G. Parisi and F. Zamponi, Rev. Mod. Phys. **82**, 789 (2010).
[24] J. P. Hansen and I. R. McDonald, *Theory of Simple Liquids*, 3rd ed. (Academic, Burlington, 2006).
[25] W. Götze, *Complex Dynamics of Glass-Forming Liquids* (Oxford University Press, Oxford, 2009).
[26] W. van Megen, T. C. Mortensen, S. R. Williams, and J. Müller, Phys. Rev. E **58**, 6073 (1998).
[27] G. Brambilla, D. El Masri, M. Pierno, L. Berthier, L. Cipelletti, G. Petekidis, and A. B. Schofield, Phys. Rev. Lett. **102**, 085703 (2009); D. El Masri, G. Brambilla, M. Pierno, G. Petekidis, A. B. Schofield, L. Berthier, and L. Cipelletti, J. Stat. Mech.: Theory Exp. (2009) P07015.
[28] L. Berthier and T. A. Witten, Phys. Rev. E **80**, 021502 (2009).
[29] E. Zaccarelli, C. Valeriani, E. Sanz, W. C. K. Poon, M. E. Cates, and P. N. Pusey, Phys. Rev. Lett. **103**, 135704 (2009).
[30] P. N. Pusey, E. Zaccarelli, C. Valeriani, E. Sanz, W. C. K. Poon, and M. E. Cates, Philos. Trans. R. Soc., A **367**, 4993 (2009).
[31] E. Zaccarelli, S. M. Liddle, and W. C. K. Poon, Soft Matter **11**, 324 (2015).
[32] D. Heckendorf, K. J. Mutch, S. U. Egelhaaf, and M. Laurati, Phys. Rev. Lett. **119**, 048003 (2017).
[33] P. N. Segrè, S. P. Meeker, P. N. Pusey, and W. C. K. Poon, Phys. Rev. Lett. **75**, 958 (1995).